SINGLE-STAGE CURRENT SOURCE INVERTER WITH AMPLIFIED SINUSOIDAL OUTPUT VOLTAGE: ANALYSIS, SIMULATION AND EXPERIMENTAL RESULTS

Lucas S. Garcia, Luiz C. de Freitas, João B. Vieira Jr, Ernane A. A. Coelho, Valdeir J. Farias and Luiz C. G. Freitas
Núcleo de Pesquisas em Eletrônica de Potência (NUPEP)
Faculdade de Engenharia Elétrica (UFU)
Uberlândia, MG, Brasil 38400-902
lucas.sg@hotmail.com, lcgfreitas@yahoo.com.br

***Abstract* –Alternative energy sources has been attracting great interest in the area of static converter development. This fact is related to issues like sustainability and the world environment, which is contributing to viability of this type of energy source. The main challenge is to develop systems that transform this DC energy in AC. Within this subject, this paper focuses the establishment of a new control strategy applied to a step-down/step-up single-stage inverter with imposed waveforms of input inductor current and output voltage. The proposed control strategy provides high voltage gain without using high frequency transformer, which contributes to weigh and size reduction of the proposed DC-AC converter structure. Theoretical analysis are presented and corroborated by experimental results of a 180W laboratory prototype.**

***Keywords* -DC-AC Converters, Current Source Inverters, Alternative Energy Sources, Single-Stage Inverters.**

I. INTRODUCTION

Currently, alternative energy sources are seen as a matter of great importance in many countries. This is due to exhaustive CO_2 emissions in the atmosphere reaching alarming levels contributing, therefore, to global warming [1]. Sustainable development policies are being put into practice, in which the use of alternative and renewable energy sources show the highest rate of increase over the non-renewable resources like coal, oil and others. It is against this background that the development of power electronics is located, more precisely in the area of static power converters [2].

Due to the high growth rate of investments towards the development and use of alternative sources of energy, power electronics finds a broad market area, for example, in the development of static converters used in power generation systems using photovoltaic panels to capture solar energy and condition it into adequate energy [3]. It is worth noting that regardless of the type of alternative energy source used (fuel cell, photovoltaic panel, eolic energy, etc.), the use of static converters, depending on the application, is essential to make it possible to use these resources.

Artigo submetido em 15/04/2011. Revisado em 26/07/2011. Aceito para publicação em 09/08/2011 por recomendação do editor João Onofre P. Pinto.

Thus, the study of static converters for application in systems based on alternative energy is divided into two classes.

- Grid-Connected: systems where generated power is injected into the distribution network;
- Stand-Alone: systems where generated power is supplied into a single load. This type of application is attractive in places of difficult access to energy distribution networks [4].

Figure 1 shows a simplified schematic block diagram illustrating the method used to process the alternative energy that is presented in continuous shape. In this figure, there are two examples of typical systems named A and B. It is observed, in both models, the presence of an intermediate stage dedicated to increase the level of voltage from the power source.

In this context, several papers have been presented making it obvious that the developed static converters present, mostly, a well-defined Boost stage in the power structure or a low or high frequency transformer which goal is to obtain an amplified output voltage for inverter connection [5-13].

Given the above, this paper has as main objective to contribute with the development of static converters with reduced size and weight through a control strategy applied to a step-down/step-up DC-AC converter that operates with totally controlled input current and output voltage. The analyzed power structure consists of a Buck - Boost converter coupled to a CSI (*Current Source Inverter*), and was targeted for application in isolated systems. It is noteworthy that there are no restrictions for application in systems connected to the mains, but is important to consider a power decoupling technique to match the oscillating output power to the constant input power supplied by a PV panel or a fuel cell [14].

The main feature observed in the proposed structure is the ability to amplify voltage ($48V_{DC}$ to $110V_{AC}$) without the presence of a pre-regulator stage and without the presence of a transformer. The high voltage gain is possible through the imposition of current in the input stage power source inverter for a reference signal generated by a microcontrolled module. The use of a CSI structure arises from the possibility of achieving instant variations of output voltage as a function only of the energy stored in the input inductor. Moreover, the CSI structure has some advantages such as the generation of sinusoidal voltage with low harmonic distortion, which makes viable its connection to the network [9], [10].

Then the paper is organized so that Section II presents the structure and operating principle of the analyzed converter,

describing in detail all steps of operation, as well as the control strategy developed. Section III defines a mathematical model applied to a computer simulation, proving the control strategy and operation of the converter. For validation, the experimental results are presented in Section IV, proving the conception of the proposed converter in practice, using demonstrative figures of the main waveforms. Finally, the main conclusions regarding the analyzed structure are presented in section V.

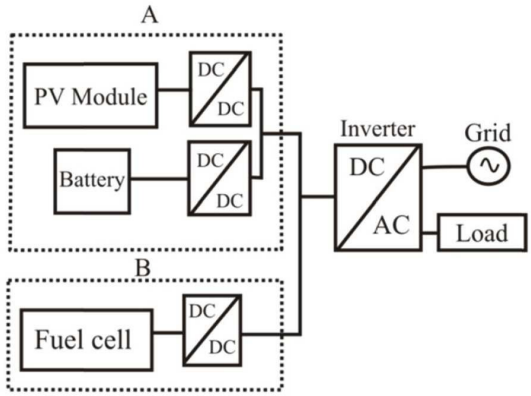

Fig.1. Schematic diagram of alternative energy systems that employ static power conversion.

II. CONVERTER DESIGN

The proposed converter is governed by a hysteresis control strategy, in which there is the imposition of two quantities: the inductor current, source of current, and voltage at the output capacitor. Many papers are presented, however, based on the imposition of control variables by means of PWM modulation techniques.

In [15] an interesting control strategy is presented by controlling the current of the Buck converter. An error signal, generated from the comparison between the reference voltage signal and output voltage signal fed back from the inverter, imposes a cyclic ratio of switch buck converter switch, and the inverter operates by simply inverting the output voltage at low frequency.

In [16] the authors present a DC-AC converter connected to the network controlled by the imposition of current in input stage, following the desired reference signal according to the possible configurations, Buck, Boost and Buck-Boost. The output voltage is controlled by PWM control.

In this context, this paper presents as the main advantage an amplified output voltage with low voltage harmonic distortion (THD_V) without an *LC* output filter and with reduced complexity of control. Depending on the acceptable rate of voltage distortion for a certain application, the control technique allows to excel better converter efficiency, benefiting from the use of alternative energy source.

A. Power Structure

The power structure basically consists of three well defined stages, which operate in parallel, and are presented in Figure 2. The topology is based on a known and reported one in the literature [15-19].

The control strategy enables complete control of input current and output voltage. One can get an output voltage with low total harmonic distortion; however this feature is linked to the efficiency of the converter.

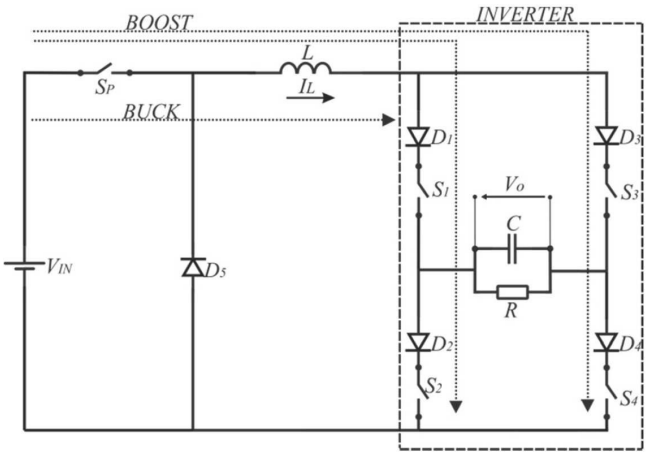

Fig.2. Operating modes of the converter.

The ideal transfer function of this converter is given in (1).

$$\frac{V_O}{V_{IN}} = \frac{D}{1-D} \tag{1}$$

B. Operating Principle

The operating principle of the proposed converter is based on the control strategy, shown in Figure 3. It is presented the power structure as well as the control logic that is done through the imposition of two variables:

- I_{REF}: Reference signal to the input current in the *L* inductor.
- V_{REF}: Reference signal to the output voltage of the capacitor *C*.

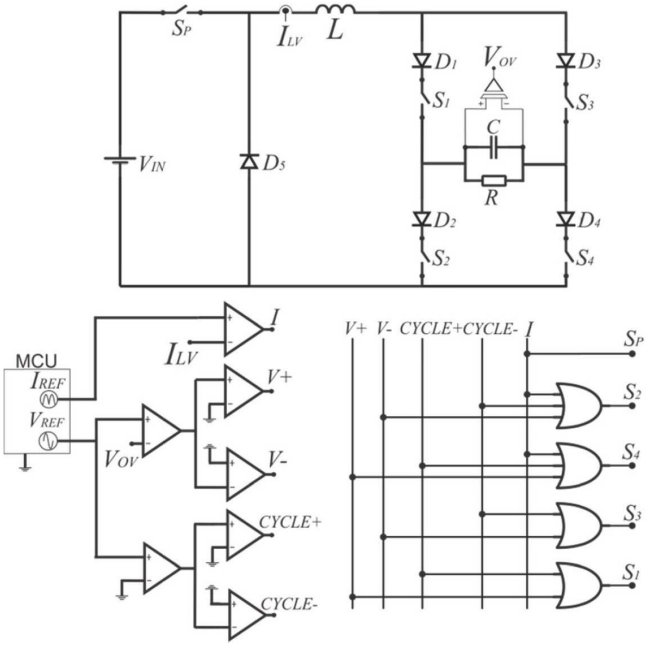

Fig.3. Control logic applied to the converter.

The control is done using a microcontrolled module, responsible for generating the reference signals, and the

analog controller, responsible for logic between the signals and transmission of control pulses to the converter.

The imposed control variables of current and voltage are shown in Figure 3 labeled I_{LV} and V_{OV} respectively. For the imposition of I_{LV} and V_{OV} the converter has three possible configurations (Boost, Buck and Buck + Boost).Thus V_{OV} follows the reference imposed by V_{REF} and I_{LV} follows the reference imposed by I_{REF}. The voltage gain, which causes the output voltage to be amplified, is given by the imposition of the I_{LV} current. In possession of certain energy, the inductor is able to provide the voltage required by the capacitor *C*.

The control strategy is defined singly. For imposition of the variables I_{REF} and V_{REF} the converter operates under the *Current Control*, described in II.*B.1* and *Voltage Control*, described in II.*B.3*, respectively. Due to the use of an inverter fed by current source it is necessary still another control that is responsible for protecting the inverter switches, since it prevents the opening of the path of circuit current. This is done by *Cycle Control*, described in II.*B.2*.

1) Current Control

This control is responsible for enforcing the desired current waveform across the inductor *L* and is shown in Figure 3 being represented by the *I* signal. The I_{LV} signal, sampled from inductor current, is compared to the reference signal I_{REF}, which is a voltage signal generated from a microcontroller and converted to analog form. The signal is a rectified sinusoidal voltage as in Figure 4. The result of the comparison between these two signals is the *I* pulse.

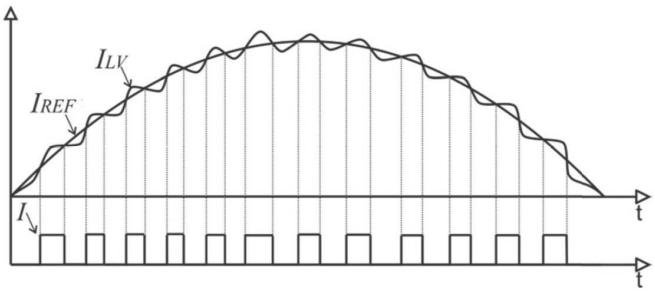

Fig.4. Imposition on the I_{LV} current shape

The control logic is governed by the following philosophy:

- $I_{REF} > I_{LV}$: *I* is a high voltage level;

In this stage of operation the S_P, S_2 and S_4 switches are activated setting the Boost mode. There are two Boost configuration modes that depend on the half cycle of converter operation. If the converter is operating in the positive half cycle the inductor current increases through the path formed by switches S_P, S_1 and S_2, as shown in Figure 5. For the negative half cycle of operation the path is formed by switches S_P, S_3 and S_4. In the Boost stage capacitor *C* provides the necessary energy to the load discharging itself through it.

- $I_{REF} < I_{LV}$: *I* is a low voltage level;

this stage of operation characterizes the Buck operation, decreasing the inductor current by transferring its energy to the inverter (Figure 7). The command *I*, in this case, the shutdown of the switches on its influence, has a direct effect only on S_P. The switches S_2 and S_4 may be being triggered by the other controls according to the control logic shown in Figure 3.

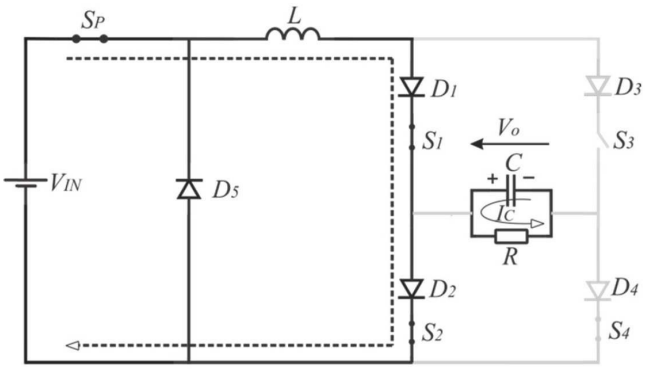

Fig.5. Boost Stage of current in positive half cycle of output voltage.

2) Cycle Control

This control is mainly intended to protect the switches of the inverter circuit. A circuit fed by current source has a characteristic such that an overvoltage occurs on the terminals of an element that disrupts current flow. The foreseen control always provides a way for the current of the inverter circuit eliminating the possibility of overvoltage across the terminals of the switches.

Another benefit occurs with the use of this control. The switches S_1 and S_3 operate at low frequency, 60Hz, reducing switching losses.

The control logic consists of the comparison between V_{REF} and ground zero, generating two pulses that are complementary as follows:

- $V_{REF} > 0$: *Cycle*+ is a high level of voltage,
  Cycle- is a low level of voltage;
- $V_{REF} < 0$: *Cycle*+ is a low voltage level,
  Cycle- is a high voltage level;

Cycle+ is maintained at a high level of voltage for the entire positive half cycle, activating the switches S_1 and S_4. *Cycle*- is maintained at a high level of voltage for the entire negative half cycle, enabling S_3 and S_2.

3) Voltage Control

This control is responsible for enforcing the waveform of the output voltage. This is done by comparing V_{REF} which is a sinusoidal voltage signal, and V_{OV}, sampled by a sensor, shown in Figure 3. The V_{REF} signal is generated by the microcontroller and is synchronized with I_{REF}.

The result of the comparison between the two signals generates two control pulses *V*+ and *V*-, which are complementary, working as follows:

- $V_{REF} > V_{OV}$: *V*+ is a high voltage level,
  V- is a low voltage level;
- $V_{REF} < V_{OV}$: *V*+ is a low voltage level,
  V- is a high voltage level;

The switches S_1 and S_4 are triggered with *V*+ and, additionally, the switches S_3 and S_2 are triggered with *V*-. The operating modes are described for the positive half cycle, so

that, for the negative half cycle the operation steps are complementary.

To $V_{REF} < V_{OV}$:

- *Cycle*+ = 1,
- *V*- = 1;

The stage of operation is shown in Figure 6. The capacitor is of the same polarity of V_O, causing the path of the inductor current, which previously was done through S_1, capacitor and S_4, changes passing through S_3, capacitor and S_2.Thus, the capacitor voltage is reduced.

In this process the circuit presents a peculiar characteristic. The capacitor, due to its instantaneous voltage polarity, becomes a voltage source to the inductor, making its current rise. Importantly, this phenomenon does not influence the efficiency of the converter, since the current I_{LV} is greater than I_{REF} deactivating the switch S_P.

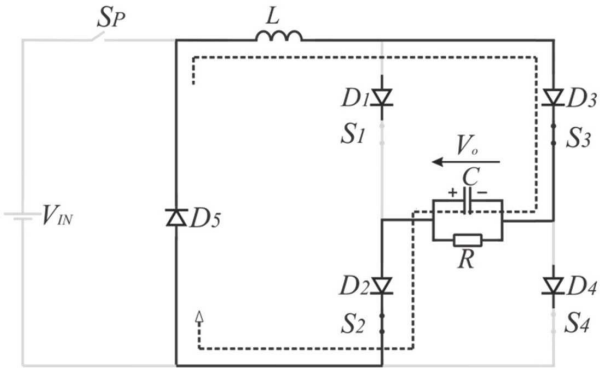

Fig.6. Operation step with *Cycle*+ and *V*-.

To $V_{REF} > V_{OV}$:

- *Cycle*+ = 1,
- *V* + = 1;

The operation stage, shown in Figure 7, is characterized by the need to increase the voltage of the capacitor. As the cycle control, which in this case already triggers the switches S_1 and S_4, *V*+ pulse has a redundant action. The energy of the inductor is then only transferred to the capacitor that ensures voltage on the load.

However, to increase the voltage on the capacitor, it is necessary that the energy in the inductor is such that provides this condition. For that, it is necessary that the current control is prioritized, with emphasis on the accumulation of energy of the inductor.

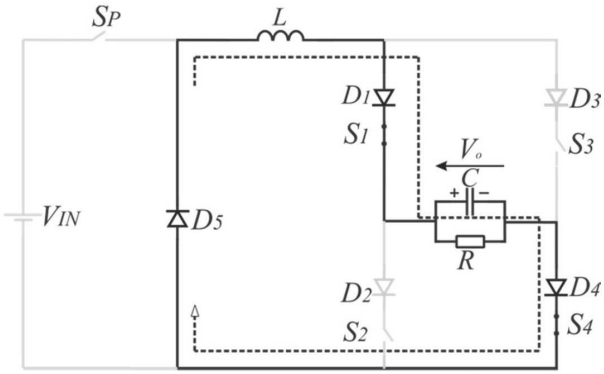

Fig.7. Operation stage with *V*+ and *Cycle*+

C. Microcontrolled Module

This module is responsible for generating reference signals, I_{REF} and V_{REF}. With the advent of the microcontroller, many different waveforms can be generated. These signals are digitally sent to a D/A converter through SPI communication, which sends the analog signal to the logic circuit as shown in Figure 8.

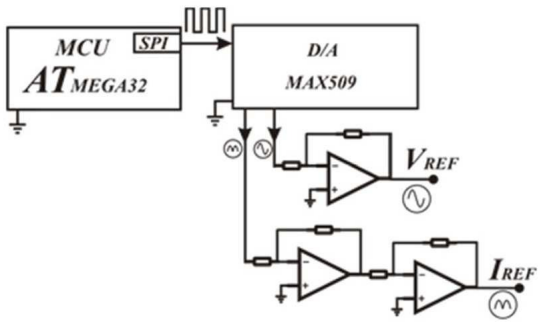

Fig.8. Microcontrolled module.

The V_{REF} signal used in this proposal is a sinusoidal signal with frequency of 60 Hz synchronized with I_{REF} which is a rectified sinusoidal signal. The need to generate two independent signals, comes from the flexibility in changing the operation of the converter.

The microcontroller allows certain features to be implemented with ease. An example can be given when it is required that the converter supplies power to a DC load or even operate with change in format and frequency of the output voltage.

III. MATHEMATICAL MODELING

The mathematical model used is based on state space, also referred to as time-domain approach. This modeling allows to represent time-varying systems and with non-zero initial conditions. The technique can be used to model systems for digital simulation. In possession of this tool, one can simulate the system and its operation dynamics by altering various input variables. This technique is attractive because many simulation softwares use it.

In general, this method is used by correctly selecting the system variables, which are called state variables, where for a system of 'n' order there will be 'n' first order differential equations. By knowing the initial condition of all state variables at time t_0 as well as the inputs of the system for $t<t_0$ one can obtain the result of the equations for $t_0>t$. The algebraic combination of state variables with the inputs of the system allows, for $t> t_0$, to obtain the output equation. The constitution of the state equations and output equations generates the representation known as system representation in states space.

The state equations can be written as follows:

$$\dot{x} = A \cdot x + B \cdot v \quad (2)$$

$$y = C \cdot x + D \cdot v \quad (3)$$

Where:

x- state vector.

$\dot{x} = \frac{dx}{dt}$ – Derivative of the state vector with respect to time;

y - response vector;

v - input or control vector;

A - system matrix;

B - input matrix;

C - output matrix;

D - forward action matrix.

A. System Definition

The state equations are obtained from circuit analysis. The system in question has eight states, which can be represented by different system and input matrices. These matrices are defined according to the configuration of the circuit breakers and are shown in Table I.

TABLE I - POSSIBLE CASES OF OPERATION OF THE CONVERTER

Case	Status		Switches Status						Action
	Cycle+	V+	I	S_P	S_1	S_2	S_3	S_4	Mode
1	0	0	0	0	0	1	1	0	BUCK
2	0	0	1	1	0	1	1	1	BOOST
3	0	1	0	0	1	1	1	1	BUCK
4	0	1	1	1	1	1	1	1	BUCK+BOOST
5	1	0	0	0	1	1	1	1	BUCK
6	1	0	1	1	1	1	1	1	BUCK+BOOST
7	1	1	0	0	1	0	0	1	BUCK
8	1	1	1	1	1	1	0	1	BOOST

Figure 9 shows the state variables in bold, I_L and V_C. V_C represents the output voltage V_O, shown in section II. Figures 10-13 show the equivalent circuits for each case of operation for the positive half cycle, named case 5 to 8, whereas for the negative half cycle the analysis is analogous.

The state vector and the derivative of the state vector can be written (4) and (5).

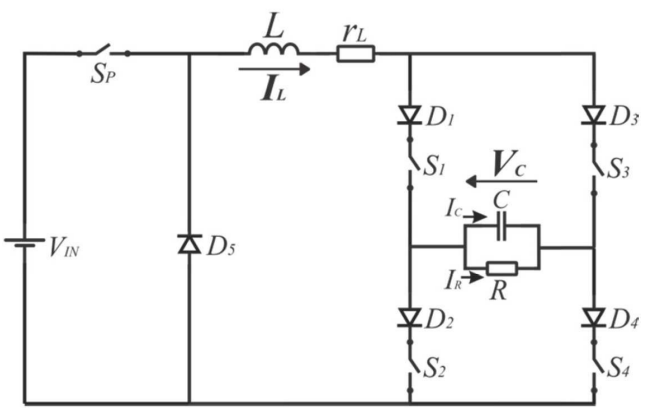

Fig.9. General diagram of the power circuit, representing the state variables in bold.

$$x_{(t)} = \begin{bmatrix} Vc \\ IL \end{bmatrix} \tag{4}$$

$$\dot{x} = \begin{bmatrix} \frac{dVc}{dt} \\ \frac{dIL}{dt} \end{bmatrix} \tag{5}$$

$$Ic = C \cdot \frac{dVc}{dt} \tag{6}$$

$$VL = L \cdot \frac{dIL}{dt} \tag{7}$$

The output equation is described in (8) as a result of load current, i.e. the current in resistor *R*. The forward action matrix in this case is zero.

$$y = \begin{bmatrix} \frac{1}{R} & 0 \end{bmatrix} \cdot \begin{bmatrix} Vc \\ IL \end{bmatrix} \tag{8}$$

The system (A) and input (B) matrices are defined according to the status of the switches and are determined in the following items, for the positive half cycle of converter functioning. This makes possible the representation of the system in the state spaces.

1) Case 5 – BUCK mode

This case represents the circuit operating in the positive half cycle. In this situation the converter operates by discharging the energy from the inductor to the capacitor through its negative load side, causing the capacitor voltage to reduce. Despite all the switches being active, the capacitor voltage reverse polarizes the diodes D_1 and D_4. Figure 10 shows the equivalent circuit of the converter, one may notice the presence of the r_L resistance which represents the internal resistance of the circuit.

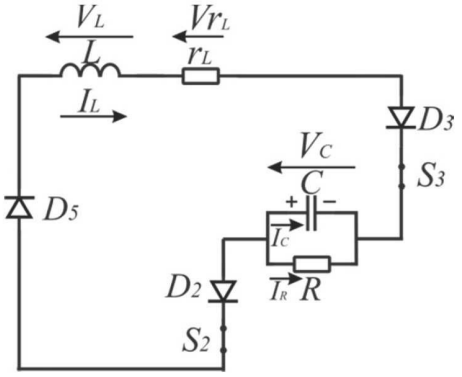

Fig.10. Equivalent circuit - case 5

From the circuit are extracted (9) and (10).

$$-VL - rL \cdot IL + Vc = 0 \tag{9}$$

$$IL = -Ic - IR \tag{10}$$

The equivalent system is shown in (11).

$$\begin{bmatrix} \frac{dVc}{dt} \\ \frac{dI_L}{dt} \end{bmatrix} = \begin{bmatrix} -\frac{1}{RC} & -\frac{1}{C} \\ \frac{1}{L} & -\frac{r}{L} \end{bmatrix} \begin{bmatrix} Vc \\ I_L \end{bmatrix} + \begin{bmatrix} 0 \\ 0 \end{bmatrix} V_{IN} \quad (11)$$

2) Case 6 – BUCK+BOOST Mode

In this situation it is necessary a decrease of the voltage on the capacitor along with the storage of energy in the inductor. It is noticed then the performance of all the switches, but the capacitor voltage reverse polarizes the diodes D_1 and D_4.The boost action occurs with the current passing through the negative side of the capacitor load, in this case the derivative of the inductor current is stronger, since it undergoes the action of two sources, the energy comes from the input V_{IN} and capacitor V_C. Figure 11 shows the equivalent circuit of the sixth operation case from Table I.

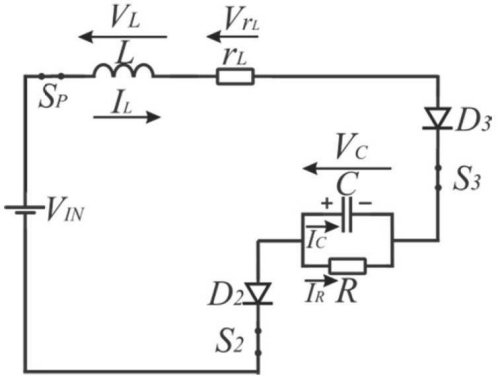

Fig.11. Equivalent circuit - case 6

In this case, there is the presence of input V_{IN}, then the B vector is not zero, making its presence to interfere with the corresponding state equation.

From the circuit are extracted (12) and (13).

$$V_{IN} - V_L - r_L \cdot I_L + Vc = 0 \quad (12)$$

$$I_L = -Ic - I_R \quad (13)$$

The equivalent system is shown in (14).

$$\begin{bmatrix} \frac{dVc}{dt} \\ \frac{dI_L}{dt} \end{bmatrix} = \begin{bmatrix} -\frac{1}{RC} & -\frac{1}{C} \\ \frac{1}{L} & -\frac{r}{L} \end{bmatrix} \begin{bmatrix} Vc \\ I_L \end{bmatrix} + \begin{bmatrix} 0 \\ \frac{1}{L} \end{bmatrix} V_{IN} \quad (14)$$

3) Case 7 – BUCK Mode

This situation represents the need to increase the voltage on the capacitor and decrease the inductor current. This occurs naturally by the energy transfer from the inductor to the capacitor.

Figure 12 shows the equivalent circuit for the seventh event of converter operation, present in Table I.

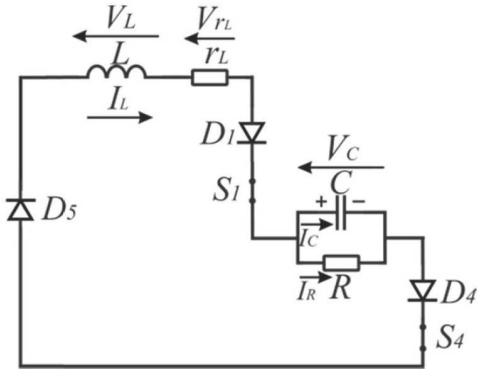

Fig.12. Equivalent circuit - case 7

From the circuit are extracted (15) and (16).

$$-V_L - r_L \cdot I_L - Vc = 0 \quad (15)$$

$$I_L = Ic + I_R \quad (16)$$

The equivalent system is shown in (17).

$$\begin{bmatrix} \frac{dVc}{dt} \\ \frac{dI_L}{dt} \end{bmatrix} = \begin{bmatrix} -\frac{1}{RC} & \frac{1}{C} \\ -\frac{1}{L} & -\frac{r}{L} \end{bmatrix} \begin{bmatrix} Vc \\ I_L \end{bmatrix} + \begin{bmatrix} 0 \\ 0 \end{bmatrix} Vin \quad (17)$$

4) Case 8 – BOOST Mode

Case 8 represents the need for increased capacitor voltage and inductor current. In this case the priority is naturally for the action of boost inductor current because although the switch S_4 is active, diode D_4 is reversely polarized by the capacitor, the path of least impedance to the circuit is done by switch S_2. Figure 13 shows the equivalent circuit.

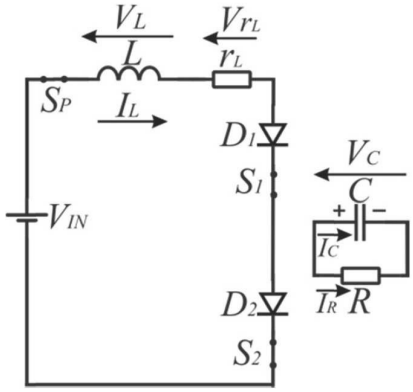

Fig.13. Equivalent circuit - case 8.

From the circuit are extracted (18) and (19).

$$V_{IN} - V_L - r_L \cdot I_L = 0 \quad (18)$$

$$Ic = I_R \quad (19)$$

The equivalent system is shown in (20).

$$\begin{bmatrix} \frac{dVc}{dt} \\ \frac{dI_L}{dt} \end{bmatrix} = \begin{bmatrix} \frac{1}{RC} & 0 \\ 0 & -\frac{r}{L} \end{bmatrix} \begin{bmatrix} Vc \\ I_L \end{bmatrix} + \begin{bmatrix} 0 \\ \frac{1}{L} \end{bmatrix} Vin \quad (20)$$

B. Computer Simulation

The computer simulation is based on a mathematical model where the systems of differential equations are solved by using mathematical methods that can be both algebraic and numeric. The simulation softwares use numerical methods for the solution of (21).

$$x_{(t)} = x_{(0)} + \int_0^t \left(A \cdot x_{(t)} + B \cdot v_{(t)} \right) dt \quad (21)$$

The computer simulation was performed by MATLAB/Simulink. The s-function block allows the solution of differential equations by iterative methods. It was used for this simulation Ode5 (Dormand-Prince) method.

The mathematical model implemented is shown in block diagram arranged in two sets, of which Figure 14 shows the master set, with input and output data related to simulation, and that can be easily accessible. These input data are sent to the subsystem. The second set presents detailing of the subsystem, which effectively represents the converter, shown in Figure 15.

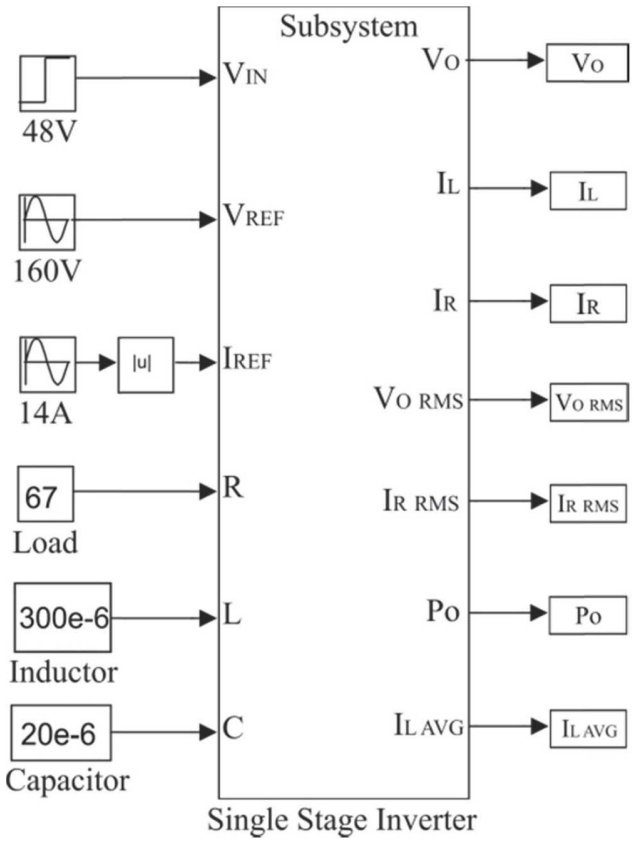

Fig.14. System representation with input and output data.

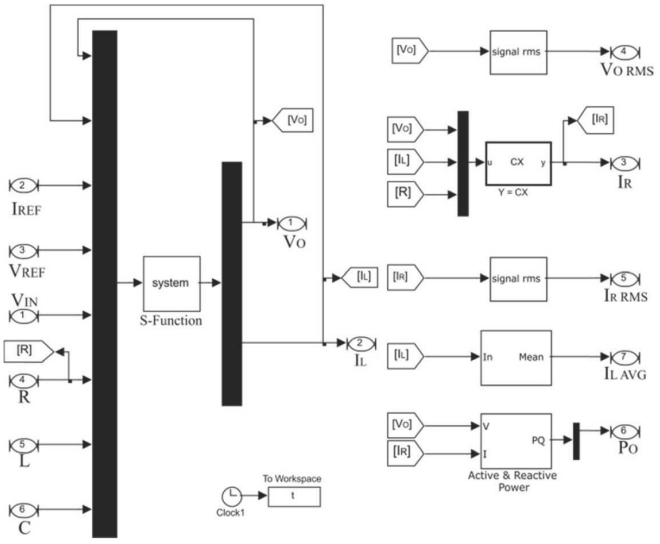

Fig.15. Diagram of the subsystem that represents, in detail, the converter from Figure 14.

The control logic presented in section II.*B* could be internally implemented in the block named system, shown in Figure 15. The result of the comparisons goes through a logic that defines which case should be taken from the ones shown in Table I. This result is saved in a control variable and is transferred to a function that returns the system of equations to be solved for the current integration step, in the form of Equation 21. Thus, it creates the state vector, which is then fed back to the next integration step.

C. Simulation Result

From the specifications shown in Table II and computational design, shown in section III.*B*, a simulation was performed.

TABLE II - SIMULATION SPECIFICATIONS

Project Specifications
Output Voltage, $V_{O\,RMS}$ = 110 V
Total Output Power, P_O = 180 W
Input Voltage, V_{IN} = 48 V_{DC}
DC-AC Converter
Input Inductor L = 300µH
Output Capacitor C = 20 µF

Figure 16 shows some results concerning the imposition of voltage. Note the output voltage V_C on capacitor with peak value at 156V, and the reference voltage used. The control strategy proves efficient for it is evident from the figure that the voltage V_C is a voltage imposed by the signal V_{REF}.

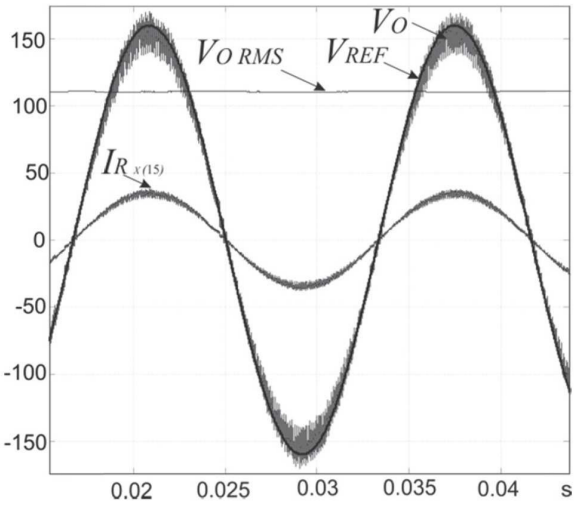

Fig.16. Results concerning the imposition of voltage.

Figure 17 shows some results concerning the imposition of current in the inductor *L*. The high current ripple occurs due to the use of a small inductor.

To make the simulation closer to reality it was necessary to emulate the behavior of an analog comparator, where there is delayed response. With this technique it is possible to observe the dynamics of the circuit, varying the elements involved in the process. One can also observe an increase in the current on approximation by zero, a phenomenon discussed in case 5 and which is complementary to the case 3 of Table I, where there is a loss of control of the inductor current as a result of the action of voltage control . Finally, it is clear the action of the current control noted by the imposition I_L based on I_{REF}.

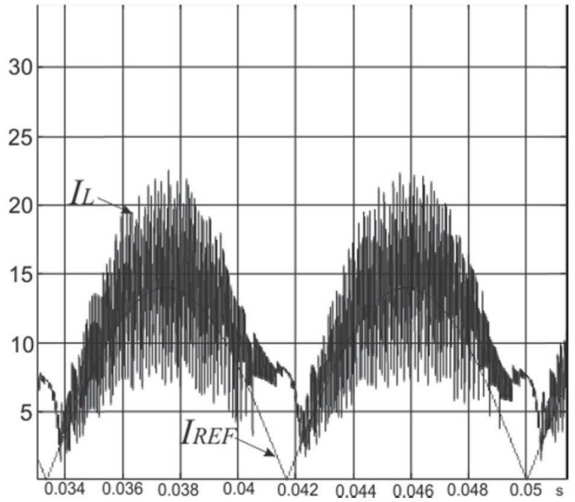

Fig.17. Results concerning the imposition of I_L current.

IV. EXPERIMENTAL RESULTS

A 180W prototype of the step-down/step-up DC-AC converter developed was built and experimentally examined in the laboratory with the intent to prove the effectiveness of the control strategy implemented and simulated. Project specifications and data from the built prototype are presented in Table III.

TABLE III - PROTOTYPE SPECIFICATIONS

Project Specifications
Output Voltage, $V_{O\,RMS}$ = 110V
Total Output Power, P_O = 180 W
Input Voltage, V_{IN} = 48 V_{DC}
DC-AC converter
Inductor *L*= 300µH, Core: 65-33-39
Capacitor *C* = 20 µF +-10%, 650 V_{AC}, 50..60Hz
Switch, S_P - S_4: IRFP264
Diodes, D_1 - D_5: STTH200L04TV
Hall Effect Voltage Sensor
Hall Effect Current Sensor
Microcontroller: ATMEGA32
D/A Converter: MAX509
Analog Comparators: LM318

Figure 18 shows a top view photo of the prototype. The switches and diodes are fixed bellow of the control circuit, at the heat sink.

Figure 19 shows the current control operation. Through the figure one can observe the phenomenon described in the voltage control, featuring the growth of I_L without the use of input voltage, V_{IN}.

The reference signal I_{REF} is shown and it is noted an increase in early and late cycle, this is due to electromagnetic interference generated by the inductor *L*.

The feedback signal I_L is subjected to a low pass filter, therefore does not represent a faithful copy of the inductor current. This technique is used, because I_L does not need to be an identical copy of its reference, but an approximation. Thus, the converter has an efficiency gain by reduction of switching losses.

Figure 20 shows the current in the inductor *L*. It is noted a high current ripple due to the reduced size of the inductor. The average value of current injected by the source is reduced since the variations are larger, reaching zero at times. It is possible to observe the phenomenon described in section II.*B.3* where there is growth of the inductor current by action of the *voltage control*.

Figure 21 shows the action of the signal *V*+ of voltage control. When V_{REF} is above sampled V_{OV}, the signal *V*+ is maintained at high level. It should be emphasized that this action does not cause the output voltage to follow the voltage imposed by the reference if there is not energy stored in the inductor *L*.

Figure 22 shows the output voltage and current with the voltage control acting, causing a sinusoidal voltage to be generated. In this condition, obtained THD_V and efficiency were 3.87% and 78% respectively. The efficiency can be improved by using semiconductor with lower conduction losses as well as employing an inductor with lower series resistance. For this application type the quality of the output voltage is within the limits recommended in IEEE 519, which limits the total harmonic distortion to 5%.

Figure 23 shows the output voltage and current without action from the voltage control. In this condition occurs only alternated voltage given by switching, at low frequency, resulting from the action of the *cycle control*. As the voltage

control does not act, there is no loss of energy to control the voltage across the output capacitor *C*. Consequently, in this operating condition, the obtained THD_V and efficiency were 20% and 86% respectively. It is noteworthy that in the context of non-isolated systems, where there is no need to maintain very low THD_V, it could be attractive since the operation of the converter without the action of voltage control presents very satisfactory results.

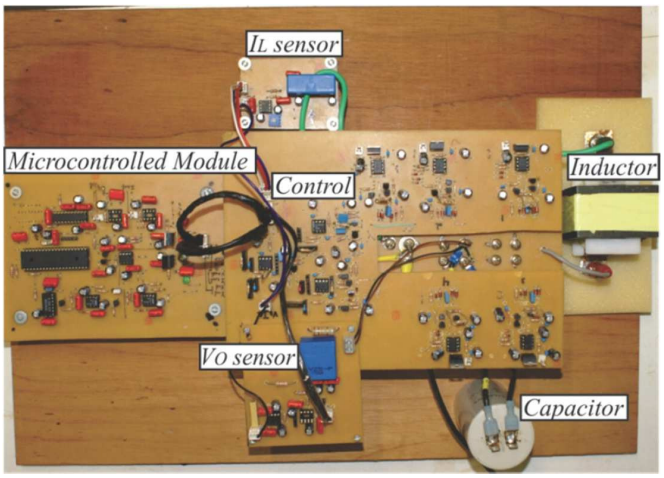

Fig.18. Photo of the 180W prototype.

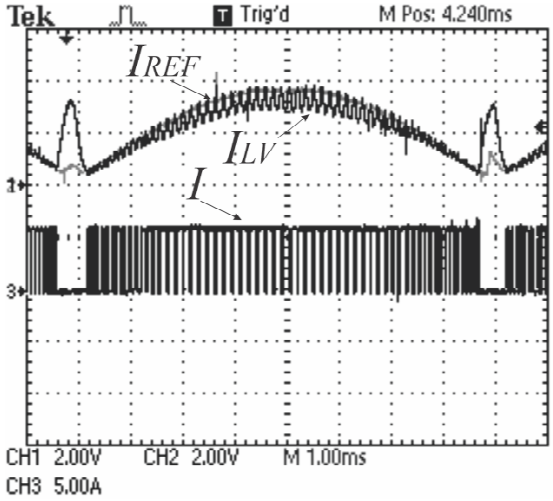

Fig.19. Experimental results of current control.

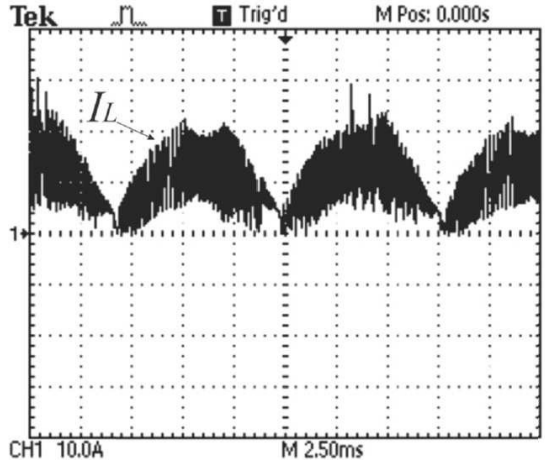

Fig.20. Current in the inductor L.

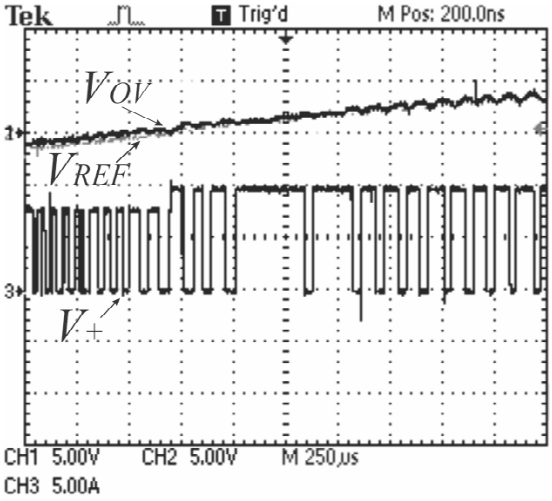

Fig.21. Action of voltage control, presenting the pulses *V*+.

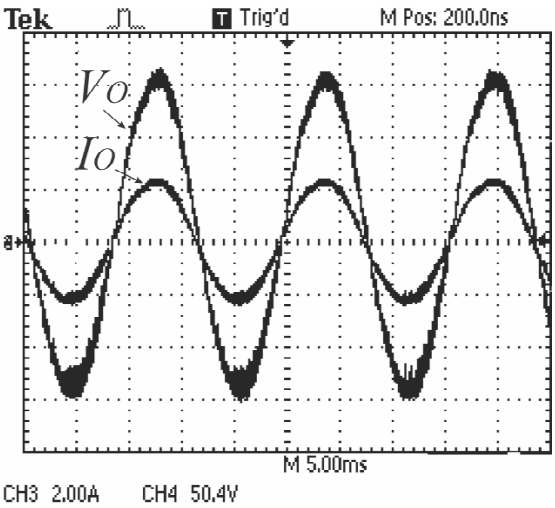

Fig.22. Output voltage and current with voltage control action, with THD_V = 3.87%.

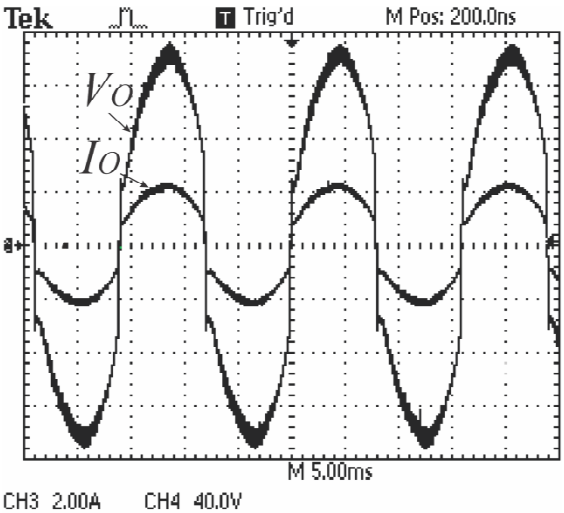

Fig.23. Output voltage and current without action from the voltage control, THD_V = 20%.

V. CONCLUSION

A step-down/step-up DC-AC converter, with input current and output voltage fully controlled feeding a single load, was presented in this paper. A high voltage gain was achieved without the use of a pre-regulator stage or a transformer, resulting in a reduced THDv.

Simulation results were presented from a mathematical model, confirming the operation proposal of the converter, and experimental results, obtained by analysis of a 180W prototype originally designed to supply stand-alone loads. Using a microcontroller for this converter provides a wide range of applications, since the reference signals can be varied. Due to the low processing level, the used microcontroller is of low cost.

The proposed converter demonstrated to be capable of generating sinusoidal voltage with low THDv. Experimental results show its high potential for applications in stand-alone systems.

ACKNOWLEDGEMENT

The authors wish to thank CAPES, CNPq and FAPEMIG for the financial support to this project.

REFERENCES

[1] International Energy Agency. (2009). World Energy Mode – Methodology and Assumptions [online]. Available: http://www.iea.org/weo/docs/weo2009/World_Energy_Model.pdf.

[2] E. Martinot, J. L. Sawin. Renewables Global Status Report: 2009 Update. REN 21 Renewable Energy policy Network for the 21st Century. Available: http://www.ren21.net/pdf/RE_GSR_2009_Update.pdf.

[3] P. K. Steimer, "Power electronics, a key techonology for future more electrical systems", *in Proc. Of IEEE Energy Conversion Congress and Exposition*, pp. 1161 – 1165, 2009.

[4] D. P. Kaundinya, P. Balachandra, N. H. Ravindranath, "Grid-connected versus stand-alone energy systems for decentralized power—A review of literature", *Renewable and Sustainable Energy Reviews 13*, pp. 2041–2050, 2009.

[5] R. O. Caceres, I. Barbi, "A boost DC-AC converter: analysis, design, and experimentation", *in IEEE Transactions on Power Electronics*, vol. 14, no. 1, pp. 134-141, Jan 1999.

[6] S. Jalbrzykowski, T. Citko, "Current-Fed Resonant Full-Bridge Boost DC/AC/DC Converter", *in IEEE Transactions on Industrial Electronics*, Vol. 55, n. 3, pp. 1198 – 1205, March 2008.

[7] I. Boonyaroonate, S. Mori, "A compact DC/AC inverter for automotive application", *ISCAS. IEEE International Symposium on*, Vol. 5, pp. V-829 – V-832, 2002.

[8] B. Kalaivani, V. K. Chinnaiyan, J. Jerome, "A novel control strategy for the boost DC - AC inverter", *in Proc. Of India International Conference on Power Electronics*, pp. 341-344, 2006.

[9] F. Gao, C. Liang, P. C. Loh, F. Blaabjerg, "Diode-Assisted Buck-Boost Current Source Inverters", *in Proc. Of 7th International Conference on Power Electronics and Drive Systems*, pp. 1187-1193, 2007.

[10] F. Kang, C. Kim, S. Park, H. Park, "Interface circuit for photovoltaic system based on buck-boost current-source PWM inverter", *in Proc. Of IEEE 28th Annual Conference of the Industrial Electronics Society*, Vol. 4, pp. 3257-3261, 2002.

[11] C. E. de A. Silva, D. de S. O. Junior, H. M. O. Filho, F. L. M. Antunes, "Dc-ac Power Supply For Battery Based Systems", *Eletrônica de Potência –SOBRAEP*, vol. 15, n. 4, pp. 255-262, Nov. 2010.

[12] S. Daher, J. Schmid, F. L. M. Antunes, "High Performance Inverter For Renewable Energy Systems", *Eletrônica de Potência –SOBRAEP*, vol. 12, n. 3, pp. 253-260, Nov 2007.

[13] R. B. Godoy, H. Z. Maia, F. J. T. Filho, L. G. Júnior, J. O. P. Pinto, G. S. Tatibana, "Projeto e Desenvolvimento de um Sistema Inversor para Fontes de Energia Renovável com Conectividade à Rede Elétrica", *Eletrônica de Potência –SOBRAEP*, vol. 12, n. 2, pp. 155-162, Jul 2007.

[14] V. S. Lacerda, P. G. Barbosa, H. A. C. Braga, "A single-phase single-stage, high power factor grid-connected PV system, with maximum power point tracking", *Industrial Technology (ICIT), IEEE International Conference on*, pp.871-877, March 2010.

[15] D. C. Martins, R. Demonti, I. Barbi, "Usage of the solar energy from the photovoltaic panels for the generation of electrical energy", *in Proc. Of The 21st International Tele-communications Energy Conference*, pp. 344-349, Jun 1999.

[16] B. S. Prasad, S. Jain, V. Agarwal, "Universal Single-Stage Grid-Connected Inverter", *in IEEE Transactions on Energy Conversion*, Vol. 23, n. 1, pp.128-137, March 2008.

[17] Z. Yang, P. C. Sen, "A novel switch-mode DC-to-AC inverter with nonlinear robust control", *in IEEE Transactions on Industrial Electronics,* Vol. 45, n. 4, pp. 602-608, Aug 1998.

[18] L. S. Garcia, L.C. de Freitas, H. J. Avelar, N. M. A. Costa, J. B. Vieira Junior, E. A. A. Coelho, V. J. Farias, L. C. G. Freitas, "Single-stage fuel-cell inverter with new control strategy," *Vehicle Power and Propulsion Conference (VPPC), 2010 IEEE* , pp.1-6, 1-3 Sept. 2010.

[19] L. S. Garcia, N. M. A. Costa, L. C. de Freitas, J. B. Vieira Junior, E. A. A. Coelho, V. J. Farias, L. C. G. Freitas, "New control strategy applied to a CSI inverter with amplified sinusoidal output voltage: Analysis, simulation and experimental results," *Energy Conversion Congress and Exposition (ECCE), 2010 IEEE*, pp. 2121-2126, Sept. 2010.

BIOGRAPHIES

Lucas Sampaio Garcia, was born in Araraquara (SP) in 1984, received the B.S., M.S. in electrical engineering 2008 and in 2010 from the Federal University of Uberlândia, Uberlândia, Brazil. Nowadays is a PhD student in the Power Electronics Research Group (NUPEP) of the same

University. His research interests includes DC-AC converters, single stage inverters and control technics involving digital features.

Luiz Carlos de Freitas, was born in Monte Alegre, Brazil, on April 1, 1952. He received the M.Sc. and Ph.D. degrees from the Universidade Federal de Santa Catarina, Florianópolis, Brazil, in 1985 and 1992, respectively. He is currently a Professor with the Faculty of Electrical Engineering, Federal University of Uberlândia, Uberlândia , Brazil . He has authored a variety of papers particularly in the areas of soft-switching, dc–dc, dc–ac, and ac–dc converters, electronic fluorescent ballasts, and multipulse power rectifier for clean-power systems. He has published in PESC'92, APEC'93, PESC'93, and IEEE TRANSACTION ON POWER ELECTRONICS (Jan. 1995), the evolution of a zero-voltage turn ON and turn OFF commutation cell that has been largely applied in power electronics research. Dr. de Freitas is a member of the Power Electronic Research Group (NUPEP) of the Federal University of Uberlândia, since 1991.

João Batista Vieira Jr. was born in Panamá, Brazil, in 1955. He received the B.S. degree in electrical engineering from the Federal University of Uberlândia, Uberlândia, Brazil, in 1980, and the M.S. and Ph.D. degrees from the Federal University of Santa Catarina, Florianópolis, Brazil, in 1984 and 1991, respectively. In 1980, he became an Instructor in the Electrical Engineering Department, Federal University of Uberlândia, where he is currently a Professor and a member of the Power Electronics Research Group (NUPEP). He has published about 300 papers. His research interests include high-frequency power conversion, modeling and control of converters, power-factor-correction circuits, and new converter topologies. Prof. Vieira is a Member of the Brazilian Automatic Society (SBA) and the Brazilian Society of Power Electronics (SOBRAEP).

ErnaneAntônioAlves Coelho was born in Teófilo Otoni-MG, Brazil, in 1962. He received the B.S. degree in Electrical Engineering from the Federal University of Minas Gerais, Belo Horizonte, Brazil, the M.S. degree from the Federal University of Santa Catarina, Florianópolis, Brazil, and the Ph.D. degree from the Federal University of Minas Gerais in 1987, 1989, and 2000, respectively. He is currently with the Power Electronics Research Group (NUPEP) in Federal University of Uberlândia, Uberlândia, Brazil. His research interests are parallel conection of PWM inverters, power factor correction, and digital control by microcontrollers and DSPs. Dr. Coelho is member of the Brazilian Society of Power Electronics (SOBRAEP).

Valdeir José Farias was born in Araguari, Brazil, in 1947. He received the B.S. degree in electrical engineering from the Federal University of Uberlândia, Uberlândia, Brazil, in 1975, the M.S. degree in power electronics from the Federal University of Minas Gerais, Belo Horizonte, Brazil, in 1981, and the Ph.D. degree from the State University of Campinas, Campinas, Brazil, in 1989. He is currently a Professor of Electrical Engineering at the Federal University of Uberlândia and a member of the Power Electronics Research Group (NUPEP). He has published about 280 papers. His research interest is power electronics, in particular, soft-switching converters and active power filters. Prof. Farias is a Member of the Brazilian Automatic Society (SBA) and the Brazilian Society of Power Electronics (SOBRAEP).

Luiz Carlos Gomes de Freitas, received the B.S., M.S., and Ph.D. degrees in electrical engineering from the Federal University of Uberlândia, Uberlândia, Brazil, in 2001, 2003, and 2006, respectively. He is currently with the Power Electronics Research Group (NUPEP), where he has been working to establish research and education activities in industry application of power electronics converters. His research interests include high-frequency power conversion, active power-factor correction techniques, multipulse rectifiers, power quality, and clean power applications. Prof. Freitas is a Member of the Brazilian Society of Power Electronics (SOBRAEP).